Available online at www.eccomasproceedia.org
Eccomas Proceedia COMPDYN (2023) 4987-4996

ECCOMAS
Proceedia

COMPDYN 2023
9th ECCOMAS Thematic Conference on
Computational Methods in Structural Dynamics and Earthquake Engineering
M. Papadrakakis, M. Fragiadakis (eds.)
Athens, Greece, 12-14 June 2023

MATRIX EQUATIONS MODELS FOR SOLVING THE DYNAMIC RESPONSE OF INELASTIC CANTILEVER STRUCTURES

Shmerling A.[1]

[1] Department of Civil and Environmental Engineering, Ben-Gurion University of the Negev
POB 653, Beer-Sheva, 84105, ISRAEL
e-mail: assafs@bgu.ac.il

Abstract

This work presents a matrix equations model approach for analyzing the dynamic response of cantilever structures. The method can be used for assessing the linear-elastic or inelastic response of buildings with a symmetric or anti-symmetric floorplan. The proposed model constitutes an alternative to finite-element analysis and a valuable tool for introducing two-dimensional and three-dimensional cantilever structures to control the theory's state-space representation and structural dynamics' equation of motion. The model regards the stiffness and mass matrices. The proposed displacement-related stiffness matrix of cantilever elements satisfies the elemental boundary conditions while deriving a symmetric stiffness matrix. The linear-elastic response analysis is performed in displacement coordinates. But, the inelastic response analysis is conducted in bending curvature coordinates to coop with smooth hysteretic models that refer to the relation between the bending moment and the bending curvature through the bending stiffness. The transformation from displacement coordinates to bending curvature coordinates is explained. In the case of buildings with an anti-symmetric floorplan, the Direct Stiffness Method (DSM) is employed to transfer the cantilever elements from their local coordinates into the global degree-of-freedom (DOF) system. The numerical accuracy of the matrix equations model is examined and showcases its reliability.

Keywords: Numerical Analysis, Cantilever Structure, Structural Dynamics, Deteriorating Inelastic Structures, Nonlinear Dynamics.

ISSN:2623-3347
Peer-review under responsibility of the organizing committee of COMPDYN 2023.
doi: 10.7712/120123.10776.21008

1 INTRODUCTION

Numerical analysis is a powerful mathematical tool used to approximate and solve complex engineering problems that are difficult to solve using analytical methods. In the case of determining the dynamic response of cantilever structures, numerical analysis techniques can be used to approximate the structural behavior of the system under dynamic loading. Typically, the cantilever structure is modeled as a finite element model, dividing the structure into a finite number of interconnected more minor elements. Each element is then analyzed separately, and the results are combined to determine the overall behavior of the structure. Several numerical analysis methods can be used for determining the dynamic response of cantilever structures, including the finite element method (FEM), the boundary element method (BEM), and the spectral element method (SEM) ([1];[2]). These methods can provide accurate predictions of the structure's dynamic behavior, such as the natural frequencies, mode shapes, and dynamic response to external loads.

One of the main downsides of FEM is the approximation error, which arises due to the discretization of the problem domain into finite elements. The accuracy of the FEM solution depends on the quality of the finite element mesh used, and a poorly designed or inaccurate mesh can lead to significant errors in the computed solutions. This issue is discussed in more detail in [3] and [4]. Another downside of FEM is the computational complexity, which arises due to the solution of an extensive system of equations. The size of the system of equations overgrows as the number of elements and degrees of freedom increases, making FEM computationally expensive and time-consuming for large-scale problems. This issue is discussed in more detail in [5] and [6]. Also, FEM may not be effective for highly nonlinear problems, as it may not accurately capture the system's complex behavior. This issue is discussed in more detail in [7] and [8]. FEM also relies on modeling assumptions, which may not accurately reflect the real-world behavior of the system. This issue is discussed in more detail in [9] and [10]. Finally, FEM can be numerically unstable for specific problems, leading to unpredictable results. This issue is discussed in more detail in [11].

One of the main disadvantages of BEM is that it is limited to problems with homogeneous boundary conditions, which restricts its applicability in certain fields such as fluid-structure interaction and acoustics. In contrast, FEM can handle problems with more general boundary conditions [12]. Another challenge of BEM is its sensitivity to the choice of fundamental solution used to represent the solution of the problem. Specifically, singularities (or nearly singularities) in the solution can result in a loss of accuracy or convergence. Additionally, BEM can be computationally expensive in certain situations, such as problems with complex geometries or nonlinear materials. This results in large matrices to solve and slow convergence of the iterative solvers [13].

One potential disadvantage of SEM is its computational cost. The method requires significant computational resources to carry out simulations accurately. This is because SEM involves using high-order polynomials to represent the solution in each element, which can lead to many degrees of freedom. As a result, SEM simulations can be more computationally expensive than other numerical methods, such as finite element methods (FEM) and finite difference methods (FDM) [14]. Another potential disadvantage of the SEM is its difficulty in handling irregular geometries. The SEM is designed to work with regular geometries, such as rectangles and cubes, which can be subdivided into elements of equal size and shape. However, irregular geometries may require more complex element shapes, leading to difficulties in the SEM. Another issue is that the SEM can suffer from "spectral pollution," leading to inaccurate solutions. Spectral pollution occurs when the high-order polynomials used in the SEM fail to represent sharp

discontinuities in the solution accurately. This can result in a loss of accuracy and convergence, particularly for problems with strong gradients or shocks ([15]).

This paper goes in a different direction and presents a matrix equations model approach for analyzing the dynamic response of cantilever structures. The method can be used for assessing the linear-elastic or inelastic response of buildings with symmetric or anti-symmetric floorplan. Accordingly, it constitutes an alternative to FEM, BEM, and SEM in case they are less feasible.

2 ANALYTICAL METHOD

2.1 Differential equation

The PDE defining the dynamic stability of a uniform cantilever element is determined. Fig 1 depicts the elevation of the element. At z=0, the horizontal displacement and slope are zero. At z=H, the distributed shear force and bending moment are zero. Hence, the lateral force equilibrium at time t at coordinate z is described by:

$$\begin{aligned} &\mathrm{m(z)\ddot{u}^{w}(z,t) + f^{R}(z,t) = p(z,t)} \\ &\mathrm{s.t.} \\ &\mathrm{0 \le z \le H} \\ &\mathrm{V^{R}(H,t) = 0} \\ &\mathrm{M^{R}(H,t) = 0} \\ &\mathrm{u^{w\prime}(0,t) = 0} \\ &\mathrm{u^{w}(0,t) = 0} \end{aligned} \tag{1}$$

Where $m(z)$ is the element characterized by distributed mass per unit length, $EI(z)$ is the distributed elasticity, $p(z,t)$ is the applied lateral load, $f^R(z,t)$ is the elemental resisting force, $u^w(z,t)$ is the lateral displacement, $\ddot{u}^w(z,t)$ is the horizontal acceleration, $M^R(z,t)$ is the distributed bending moment, and $V^R(z,t)$ is the distributed shear force.

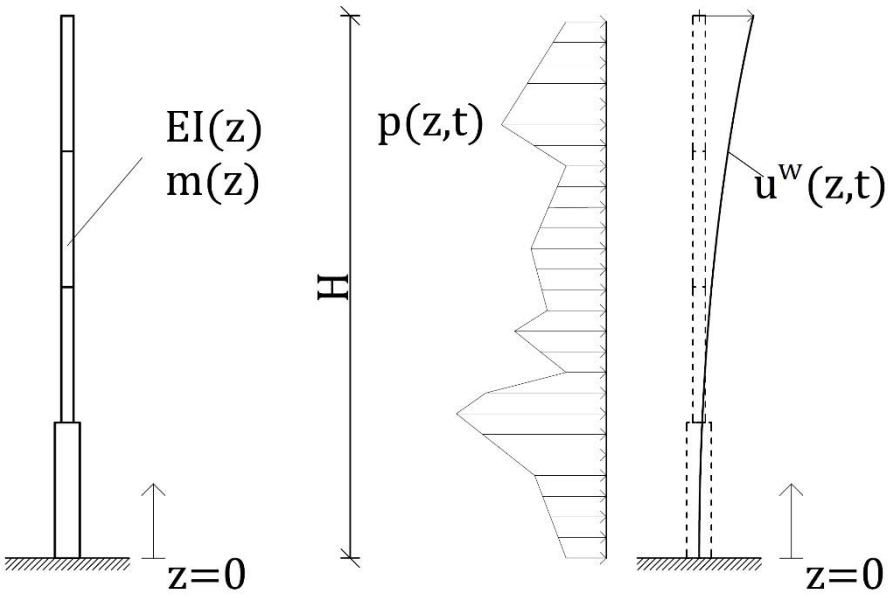

Figure 1: Cantilever element scheme

The bending moment corresponds to the distributed shear force and resisting force through the following terms:

$$V^R(z,t) = \partial M^R(z,t)/\partial z \tag{2}$$

$$f^R(z,t) = \partial^2 M^R(z,t)/\partial z^2 \tag{3}$$

Also, neglecting the shear stain in the axial stress-strain relationship provides:

$$M^R(z,t) = EI(z)u^{w\prime\prime}(z,t) \tag{4}$$

Hence, Eqs. (3) and (4) provide:

$$f^R(z,t) = \partial\big(EI(z)\varphi(z,t)\big)/\partial z^2 \tag{5}$$

Substituting Eq. (5) into Eq. (1) while using linear system modal analysis composition of the form:

$$u^w(z,t) = \sum_{v=1}^{\infty} \phi_v(z) q_v(t) \tag{6}$$

Yields the differential equation that governs the lateral motion of the cantilever element::

$$\left.\begin{array}{l} m(z)\sum_{v=1}^{\infty}\phi_v(z)\ddot{q}_v(t) + \sum_{v=1}^{\infty} F_v(z) q_v(t) = p(z,t) \\ s.t. \\ 0 \le z \le H \\ F_V(z) = \partial\big(EI(z)\phi_v''(z)\big)/\partial z^2 \\ EI(H)\phi_v{}^{(3)}(H) = 0 \\ EI(H)\phi_v{}''(H) = 0 \\ \phi_v{}'(0) = 0 \\ \phi_v(0) = 0 \end{array}\right\} \quad \forall \quad v = 1, \dots, \infty \tag{7}$$

Where $F_V(z)$ is the vth modal resisting spatial force function, $q_v(t)$ governs the vth modal system's dynamic response, and $\phi_v(z)$ is the vth modal spatial function.

2.2 Modal analysis using structural matrices

Eq. (7) is addressed and analyzed using the matrix model developed by this paper instead of assuming a general solution function. Define the relationship between $\phi_v(z)$ and $F_V(z)$ through the function $k^{-1}(z)$, which resembles the elemental flexibility distribution. That is:

$$\phi_v(z) = k^{-1}(z)\, F_v(z) \quad \forall \quad v = 1, \dots, \infty \tag{8}$$

In essence, such a function is a quad integration operator of the form:

$$k^{-1}(z) \equiv \iint \frac{1}{EI(z)} \iint dz dz dz dz \tag{9}$$

However, it should count for the boundary conditions of Eq. (7). In the case of the cantilever element, since the homogenous set of boundary condition equations relates to four different derivative orders, the conditions can all be satisfied by calculating the following integration limitations:

$$\begin{aligned}
&\int_H^z \mathrm{F_v}(z)dz = \mathrm{EI(z)}\phi_\mathrm{v}{}^{(3)}(\mathrm{z}) && \leftrightarrow \quad \mathrm{EI(H)}\phi_\mathrm{v}{}^{(3)}(\mathrm{H}) = 0\\
&\int_H^z \int_H^z \mathrm{F_v}(z)dz\,dz = \mathrm{EI(z)}\phi_\mathrm{v}{}''(\mathrm{z}) && \leftrightarrow \quad \mathrm{EI(H)}\phi_\mathrm{v}{}''(\mathrm{H}) = 0\\
&\int_0^z \frac{1}{EI(z)} \int_H^z \int_H^z \mathrm{F_V}(z)dz\,dz\,dz = \phi_\mathrm{v}{}'(\mathrm{z}) && \leftrightarrow \quad \phi_\mathrm{v}{}'(0) = 0\\
&\int_0^z \int_0^z \frac{1}{EI(z)} \int_H^z \int_H^z \mathrm{F_V}(z)dz\,dz\,dz\,dz = \phi_\mathrm{v}(\mathrm{z}) && \leftrightarrow \quad \phi_\mathrm{v}(0) = 0
\end{aligned} \tag{10}$$

That is:

$$\mathrm{k^{-1}(z)} = \int_0^\mathrm{z} \int_0^\mathrm{z} \frac{1}{\mathrm{EI}(z)} \int_\mathrm{H}^\mathrm{z} \int_\mathrm{H}^\mathrm{z} \mathrm{F_v}(z)\mathrm{d}z\,\mathrm{d}z\,\mathrm{d}z\,\mathrm{d}z \quad \forall \quad \mathrm{v} = 1,2,\ldots,\infty \tag{11}$$

Numerical integration is now utilized to define the matrix representation of $k^{-1}(z)$ (i.e., the flexural matrix) while accounting for its symmetricity. The matrix corresponds to a mesh size of Δz and is denoted as:

$$\mathbf{k}_{\Delta\mathrm{z}}{}^{-1} = \mathbf{T}_{z\in[0\to\mathrm{z}]}^{\int \mathrm{d}z}\, \mathbf{T}_{z\in[0\to\mathrm{z}]}^{\int \mathrm{d}z}\, (\mathbf{EI}_{\Delta\mathrm{z}})^{-1}\, \mathbf{T}_{z\in[\mathrm{H}\to\mathrm{z}]}^{\int \mathrm{d}z}\, \mathbf{T}_{z\in[\mathrm{H}\to\mathrm{z}]}^{\int \mathrm{d}z} \tag{12}$$

Given that the mesh size yields an $N=H/\Delta z$ grid, the matrix $\mathbf{EI}_{\Delta z}$ is diagonal and defined as:

$$\mathbf{EI}_{\Delta\mathrm{z}} = \Delta\mathrm{z}\ \mathrm{diag}\{\mathrm{EI}(0) \quad \cdots \quad \mathrm{EI}(\mathrm{n}\,\Delta\mathrm{z}) \quad \cdots \quad \mathrm{EI}(\mathrm{N}\,\Delta\mathrm{z})\} \tag{13}$$

The symmetricity of $\mathbf{k}_{\Delta z}{}^{-1}$ is provided by employing the Riemann Left Sum (RLS) scheme, which corresponds to the following transformation matrices:

$$\mathbf{T}_{z\in[0\to\mathrm{z}]}^{\int \mathrm{d}z} = \Delta\mathrm{z}\begin{bmatrix} 0 & 0 & 0 & \cdots & 0 & 0 & 0\\ 1 & 0 & 0 & \cdots & 0 & 0 & 0\\ 1 & 1 & 0 & \cdots & 0 & 0 & 0\\ \vdots & \vdots & \vdots & \ddots & \vdots & \vdots & \vdots\\ 1 & 1 & 1 & \cdots & 0 & 0 & 0\\ 1 & 1 & 1 & \cdots & 1 & 0 & 0\\ 1 & 1 & 1 & \cdots & 1 & 1 & 0 \end{bmatrix}_{\mathrm{N+1\times N+1}} \cong \int_0^\mathrm{z} \mathrm{d}z \tag{14}$$

$$\mathbf{T}_{z\in[\mathrm{H}\to\mathrm{z}]}^{\int \mathrm{d}z} = -\Delta\mathrm{z}\begin{bmatrix} 0 & 1 & 1 & \cdots & 1 & 1 & 1\\ 0 & 0 & 1 & \cdots & 1 & 1 & 1\\ 0 & 0 & 0 & \cdots & 1 & 1 & 1\\ \vdots & \vdots & \vdots & \ddots & \vdots & \vdots & \vdots\\ 0 & 0 & 0 & \cdots & 0 & 1 & 1\\ 0 & 0 & 0 & \cdots & 0 & 0 & 1\\ 0 & 0 & 0 & \cdots & 0 & 0 & 0 \end{bmatrix}_{\mathrm{N+1\times N+1}} \cong -\int_\mathrm{H}^\mathrm{z} \mathrm{d}z \tag{15}$$

Accordingly, the general form of the derived $\mathbf{k}_{\Delta z}{}^{-1}$ is:

$$\mathbf{k}_{\Delta\mathrm{z}}{}^{-1} = \begin{bmatrix} \mathbb{Z}_{2\times 2} & \mathbf{0}_{2\times N-1} \\ \mathbf{0}_{N-1\times 2} & \boldsymbol{\mathcal{F}}_{\Delta\mathrm{z}} \end{bmatrix} \tag{16}$$

In Eq. (16), $\mathbb{Z}$ is a 2×2 diagonal matrix whose components are close to zero.

The inverse of $\mathbf{k}_{\Delta z}{}^{-1}$ resembles the stiffness matrix of the cantilever element and is defined by the expression:

$$\mathbf{k}_{\Delta\mathrm{z}} = \begin{bmatrix} \boldsymbol{\Lambda} & \mathbf{0}_{2\times N-1} \\ \mathbf{0}_{N-1\times 2} & (\boldsymbol{\mathcal{F}}_{\Delta\mathrm{z}})^{-1} \end{bmatrix} \quad \leftrightarrow \quad \boldsymbol{\Lambda} = \begin{bmatrix} \Lambda_1 & 0 \\ 0 & \Lambda_2 \end{bmatrix} \equiv \begin{bmatrix} \infty & 0 \\ 0 & \infty \end{bmatrix} \tag{17}$$

So that $\boldsymbol{\Lambda}$ a 2×2 diagonal matrix whose components are of a large magnitude that simulates infinity. Also, the mass matrix of the cantilever element may be defined as:

$$\mathbf{m}_{\Delta z} = \Delta z \, \mathrm{diag}\left\{\frac{m(0)}{2} \quad m(\Delta z) \quad \cdots \quad m(n\,\Delta z) \quad \cdots \quad m\big((N-1)\,\Delta z\big) \quad \frac{m(N\,\Delta z)}{2}\right\} \tag{18}$$

Having defined the stiffness and mass matrix, the modal frequencies and modal shape vectors stem from the eigenvalue problem:

$$\det\left|\mathbf{m}_{\Delta z}{}^{-1}\mathbf{k}_{\Delta z} - \omega_{\Delta z,v}{}^{2}\mathbf{I}\right| = 0 \quad \leftrightarrow \quad \omega_{\Delta z,1} < \omega_{\Delta z,2} < \cdots \omega_{\Delta z,N+1} \tag{19}$$

$$\left(\mathbf{m}_{\Delta z}{}^{-1}\mathbf{k}_{\Delta z} - \omega_{\Delta z,v}{}^{2}\mathbf{I}\right)\boldsymbol{\phi}_{\Delta z,v} = \mathbf{0} \quad \forall \quad v = 1,2,\ldots,\infty \tag{20}$$

2.3 Numerical accuracy

The numerical accuracy of the matrix equations model is exemplified by referring to the modal frequencies of a cantilever element of uniform mass per unit length $m(z)=m$ and constant elasticity function $EI(z)=EI$. Using the analytical solution provided in chapter 17 in [16], we have the following exact terms for ω_v and $\phi_v(z)$:

$$\omega_v = \frac{(\varepsilon_v H)^2}{H^2}\sqrt{\frac{EI}{m}} \quad \forall \quad v = 1,2,\ldots,\infty \tag{21}$$

$$\phi_v(z) = C_v\left[\cosh(\varepsilon_v z) + \cos(\varepsilon_v z) + \frac{\cosh(\varepsilon_v H)-\cos(\varepsilon_v H)}{\sinh(\varepsilon_v H)-\sin(\varepsilon_v H)}\left(\sinh(\varepsilon_v z) - \sin(\varepsilon_v z)\right)\right] \tag{22}$$

So that $\varepsilon_v H$ stems from:

$$1 + \cos(\varepsilon_v H)\cosh(\varepsilon_v H) = 0 \quad \leftrightarrow \quad 0 < \varepsilon_1 H < \varepsilon_2 H < \cdots < \varepsilon_v H < \cdots \tag{23}$$

The examination herein observes the first six modal systems and employs eight mesh-size cases of Δz={H/8000; H/4000; H/2000; H/1000; H/500; H/200; H/100; H/50; H/20; H/10} so that the corresponding number of lateral DOFs is N+1={8001; 4001; 2001; 1001; 501; 201; 101; 51; 21; 11}. The results for err($\omega_{\Delta z,v}$) and err($\phi_{\Delta z,v}(H)$) versus $\Delta z/H$ are depicted in Figures 2 and 3, respectively. Figure 2 shows that for $\Delta z/H$<0.01, the relative error decreases linearly with $\Delta z/H$, while Figure 3 shows the same for $\Delta z/H$<0.002. It can also be concluded that for err( )<0.01, a mesh size of $\Delta z/H$<0.01 is recommended. Lastly, the figures exemplify that the numerical accuracy is deterred for $\Delta z/H$<0.0005

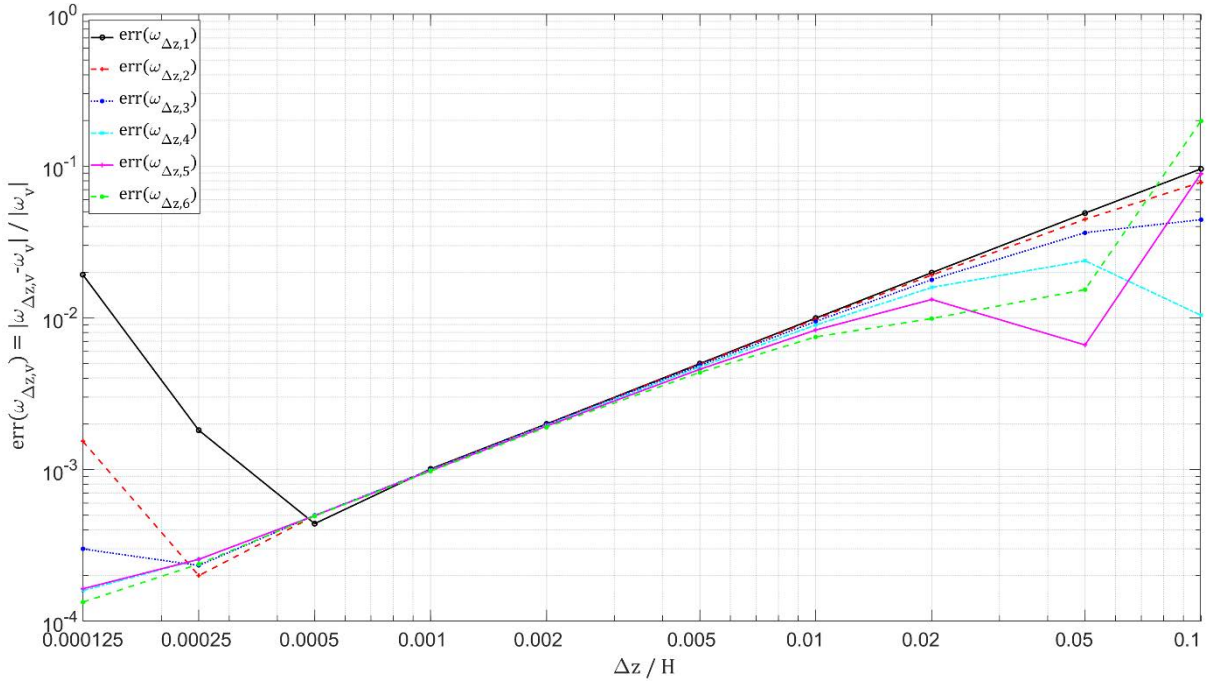

Figure 2: Modal frequency error

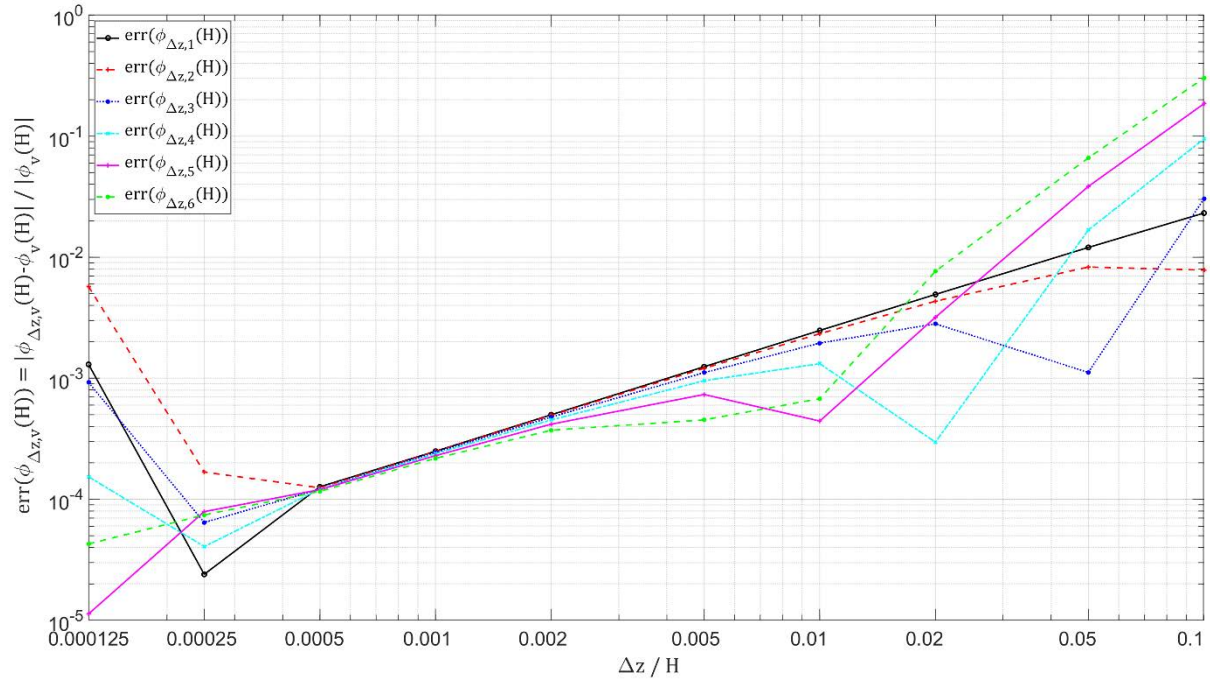

Figure 3: Modal spatial function error

3 INELASTIC ANALYSIS

The inelasticity of the cantilever structure can be introduced to the stiffness matrix using smooth hysteretic models, for example, the model presented by [17]. The model implementation approach is detailed in [18]. Most hysteretic models refer to the behavior of the bending moment instead of the lateral force equilibrium. Consequently, the cantilever element is analyzed in bending-curvature coordinates.

When working in bending coordinates, the stiffness matrix becomes:

$$\mathbf{k}^*_{\Delta z} = \Delta z \, \mathrm{diag}\left\{\frac{EI(0)}{2} \quad EI(\Delta z) \quad \cdots \quad EI(n\,\Delta z) \quad \cdots \quad EI\big((N-1)\,\Delta z\big) \quad \frac{EI(N\,\Delta z)}{2}\right\} \tag{24}$$

And the mass matrix becomes:

$$\mathbf{m}^*_{\Delta z} = \mathbf{T}^{\int dz}_{z\in[H\to 0]}\mathbf{T}^{\int dz}_{z\in[H\to 0]}\mathbf{m}_{\Delta z}\mathbf{T}^{\int dz}_{z\in[0\to H]}\mathbf{T}^{\int dz}_{z\in[0\to H]} \tag{25}$$

The elemental inelasticity is applied to the components of $\mathbf{k}^*_{\Delta z}$.

4 THREE-DIMENSIONAL STRUCTURES

The structural matrices representing the cantilever element's mass and stiffness can be used to analyze buildings with anti-symmetric floorplan (i.e., three-dimensional structures). The Direct Stiffness Method (DSM) adds elements to the global matrices, and the building is addressed as a whole. Such implementation is exemplified in [18]. The three-dimensional model refers to the Euler-Bernoulli assumption, so the ceilings are considered rigid diaphragms of zero mutuality between the horizontal *x* and *y* directions. The elements have no movement in the z-direction.

The DSM transformation matrices, from local coordinates into the building's global coordinates, are:

$$\mathbf{a}_{k,x} = \begin{bmatrix} 1 & & \rho_{xy,0} & & & -\Delta y_0 & & \\ & \ddots & & \ddots & & & \ddots & \\ & & 1 & & \rho_{xy,N} & & & -\Delta y_N \end{bmatrix}^T \tag{26}$$

$$\mathbf{a}_{k,y} = \begin{bmatrix} \rho_{yx,0} & & & 1 & & \Delta x_0 & & \\ & \ddots & & & \ddots & & \ddots & \\ & & \rho_{yx,N} & & & 1 & & \Delta x_N \end{bmatrix}^T \tag{27}$$

So that Δy_n is the distance between the center of the cantilever element and the DOFs origin in the *y*-direction, Δx_n is the distance between the center of the cantilever element and the DOFs origin in the *x*-direction, $\rho_{xy,n}$ is the stiffness mutuality from the x-direction to the y-direction at the n^{th} DOF level, and $\rho_{yx,n}$ is stiffness mutuality from the y-direction to the x-direction at the n^{th} DOF level. Accordingly, the global stiffness matrix is defined by:

$$\mathbf{K}_{\Delta z} = \sum \mathbf{a}_{k,x}\mathbf{k}_{\Delta z,x}\mathbf{a}_{k,x} + \sum \mathbf{a}_{k,y}\mathbf{k}_{\Delta z,y}\mathbf{a}_{k,y} \tag{28}$$

Here, $\mathbf{k}_{\Delta z,x}$ denotes the elemental stiffness in the x-direction, and $\mathbf{k}_{\Delta z,y}$ represents the stiffness in the *y*-direction.

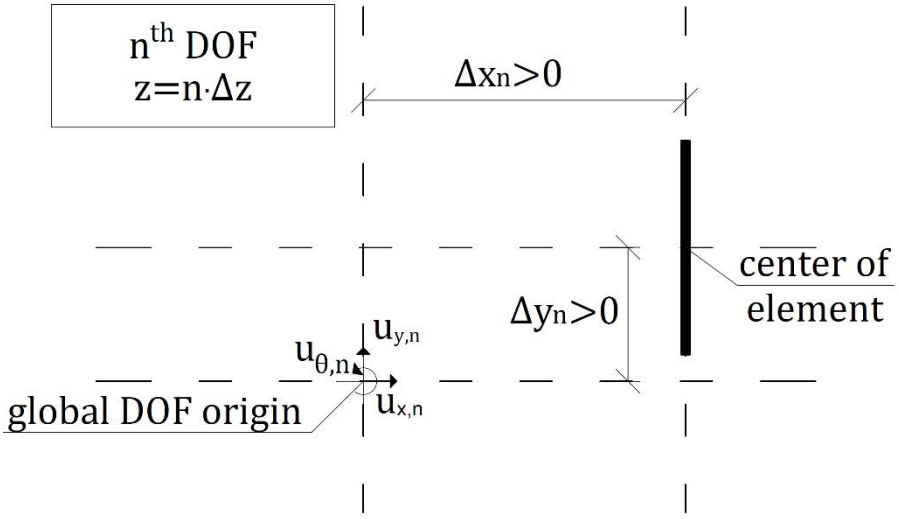

Figure 4: Distance depiction and sign

5 CONCLUSIONS

The paper presents an alternative approach to the dynamic analysis of inelastic structures with cantilever load-carrying elements. The partial differential equation governing the lateral motion and the boundary conditions of a cantilever element is described and added with modal superposition. Then, the relationship between the modal resisting force and the modal spatial function is defined and addressed through the flexibility function.

The flexibility function is, in essence, a quad integration operator that counts for the boundary condition. Since the homogenous set of boundary condition equations of a cantilever element refers to four different derivative orders of the lateral displacement function, numerical integration is applied to satisfy all conditions uniquely. Also, The LRS method is employed to yield a symmetric flexibility matrix. The flexibility matrix is then inverted into the stiffness matrix representing the elemental resistance to lateral dynamic load. The stiffness and mass matrices are employed in the three-dimensional analysis using the DSM and inelastic response analysis using continuous hysteretic models.

The numerical accuracy of the proposed approach is examined and presented in terms of modal frequencies and spatial functions. For $\Delta z/H<0.01$, the relative error decreases linearly with $\Delta z/H$, and the numerical accuracy is reduced for $\Delta z/H<0.0005$. These results indicate that the matrix equations model offers a solid and reliable method for analyzing buildings with cantilever elements using matrix equations.

REFERENCES

[1] T. Chandrupatla, A. Belegundu, *Introduction to Finite Elements in Engineering.* Pearson Education, 2021.

[2] T.J.R. Hughes, *The finite element method: linear static and dynamic finite element analysis.* Courier Corporation, 2012.

[3] O.C. Zienkiewicz, R.L. Taylor, *The finite element method for solid and structural mechanics.* Elsevier, 2005.

[4] K.J. Bathe, *Finite element procedures.* Prentice-hall New Jersey, 1996.

[5] T.J.R. Hughes, *The finite element method: linear static and dynamic finite element analysis.* Courier Corporation, 2012.

[6] J.N. Reddy, *An Introduction to the Finite Element Method,* McGraw-Hill. Inc., New York, 1993.

[7] P. Wriggers, *Nonlinear finite element methods.* Springer Science & Business Media, 2008.

[8] T. Belytschko, W.K. Liu, B. Moran, K. Elkhodary, *Nonlinear finite elements for continua and structures.* John Wiley & sons, 2014.

[9] X. Chen, Y. Liu, *Finite element modeling and simulation with ANSYS Workbench.* CRC press, 2018.

[10] J.S. Przemieniecki, *Theory of matrix structural analysis.* Courier Corporation, 1985.

[11] J. Donea, A. Huerta, *Finite element methods for flow problems.* John Wiley & Sons, 2003.

[12] J.T. Katsikadelis, *The boundary element method for engineers and scientists: theory and applications.* Academic Press, 2016.

[13] F. Paris, J. Canas, *Boundary element method: fundamentals and applications.* Oxford University Press, USA, 1997.

[14] G.E. Karniadakis, G. Karniadakis, S. Sherwin, *Spectral/hp element methods for computational fluid dynamics.* Oxford University Press on Demand, 2005.

[15] A.T. Patera, A spectral element method for fluid dynamics: laminar flow in a channel expansion. *J. Comput. Phys*. **54**, 468–488, 1984.

[16] A.K. Chopra, Dynamics of Structures 5th Edition, *Prentice-hall International Series*, 2016.

[17] M. V. Sivaselvan, A. M. Reinhorn, Hysteretic models for deteriorating inelastic structures. *J. Eng. Mech*. **126**, 633–640, 2000.

[18] A. Shmerling, Matrix equations models for nonlinear dynamic analysis of two-dimensional and three-dimensional RC structures with lateral load resisting cantilever elements. *Nonlinear Dyn.* **111**, 493–528 (2023).